Light Emission from Silicon: Some Perspectives and Applications

A.T. FIORY[1] and N.M. RAVINDRA[1,2]

1.—Department of Physics, New Jersey Institute of Technology, Newark, NJ 07102. 2.—E-mail: ravindra@njit.edu

Research on efficient light emission from silicon devices is moving toward leading-edge advances in components for nano-optoelectronics and related areas. A silicon laser is being eagerly sought and may be at hand soon. A key advantage is in the use of silicon-based materials and processing, thereby using high yield and low-cost fabrication techniques. Anticipated applications include an optical emitter for integrated optical circuits, logic, memory, and interconnects; electro-optic isolators; massively parallel optical interconnects and cross connects for integrated circuit chips; lightwave components; high-power discrete and array emitters; and optoelectronic nanocell arrays for detecting biological and chemical agents. The new technical approaches resolve a basic issue with native interband electro-optical emission from bulk Si, which competes with nonradiative phonon- and defect-mediated pathways for electron-hole recombination. Some of the new ways to enhance optical emission efficiency in Si diode devices rely on carrier confinement, including defect and strain engineering in the bulk material. Others use Si nanocrystallites, nanowires, and alloying with Ge and crystal strain methods to achieve the carrier confinement required to boost radiative recombination efficiency. Another approach draws on the considerable progress that has been made in high-efficiency, solar-cell design and uses the reciprocity between photo- and light-emitting diodes. Important advances are also being made with silicon-oxide materials containing optically active rare-earth impurities.

Key words: Silicon LED, optoelectronics, electroluminescence

INTRODUCTION

The quest for silicon-based light-emitting devices is being motivated by numerous potential applications for Si light-emitting diodes (LEDs) and lasers. An optical emitter would be a component in integrated optical circuits with logic, memory, and interconnect functionalities. Silicon-based planar waveguides are a particular application. Silicon optical emitters can also be deployed in massively parallel optical interconnects and cross connects for microprocessor and digital-signal processor applications and for lightwave components. They would be used in high-power and discrete array emitters and optical-based, nanocell detector arrays. Key advantages of Si-based materials and processing are the high yield and low production cost established in microelectronics, such as in foundry fabrication facilities for silicon integrated circuits.

Silicon has traditionally been regarded as a difficult semiconductor candidate for light emission, owing to the indirect bandgap of the bulk crystal. However, much work has shown that light emission from silicon and silicon-compatible materials is readily obtained. In this paper, we review the diversity of approaches recently taken to circumvent the physical limitation of silicon, when compared to direct bandgap semiconductors.

Phonon-mediated light emission from bulk Si is a three-particle interaction, and exciton formation and annihilation can also be involved. The mechanism is the inverse of the photoelectric effect, which was observed at the time of the discovery of the silicon p-n junction over 60 years ago.[1,2] The desir-

(Received May 30, 2003; accepted June 30, 2003)

able light-emission process involves the bimolecular radiative-recombination coefficient, $\beta = 3 \times 10^{15}$ cm^{-3} s^{-1}. The competing undesirable processes are Shockley–Read–Hall nonradiative recombination, which is material dependent and expressed by a lifetime, $\tau_{NR} \sim 10^{-5}$–10^{-3} s, and Auger recombination, given by the coefficient, $\gamma \approx 10^{-30\pm0.5}$ cm^{-6} s^{-1}. Under high injection, where the electron concentration, n, is on the order of the hole concentration, p, the theoretical, internal quantum efficiency is expressed as $\eta \approx \beta\, n\, (\tau_{NR}{}^{-1} + \beta\, n + \gamma\, n^2)^{-1}$, which can approach 1%. While this is sufficiently high efficiency for device applications, a bulk-Si p-n junction LED has a slow response time that is limited by the relaxation time for phonon absorption and emission.

Silicon-based light-emitting devices reported in the literature have exploited a variety of light-emission mechanisms and fabrication methods. Performance is generally gauged by a measurement of the external quantum efficiency of light emission, which is generally less than the internal quantum efficiency.

INTERBAND LIGHT EMISSION

Several routes to optimized, Si LED devices based on p-n recombination have been investigated. These include light-trapping cell designs, selection of silicon materials with high nonradiative-recombination lifetimes, carrier and excitonic confinement and quantum confinement, and the use of structures to enable bypassing phonon mediation altogether. Progress in the quest for a silicon laser has recently been the subject of a review.[3]

Reduced Dimensional Structures

When silicon is fabricated as small clusters, thin wires, and thin layers, band structure modifications lead to energy gaps that generally increase with decreasing cluster size, wire diameter, and layer thickness.[4] Quantum confinement theory may explain some of the luminescence observations in porous silicon, where etching produces fine features in the form of needles, clusters, and other shapes.[5]

Quantum confinement in one dimension, which is produced in ultra-thin silicon films, modifies the conduction- and valence-band edges and provides a means for bandgap engineering. In a well-controlled experimental study of quantum effects on band edges, crystalline-silicon quantum wells bounded by SiO_2 were prepared by an epitaxial transfer silicon-on-insulator (SOI) process.[6] Owing to their being widely used in the fabrication of microelectronic integrated circuits, SOI wafers are regarded as viable media for silicon nanoelectronics and optoelectronics. For films of various thicknesses, conduction-band minima were measured by x-ray absorption near-edge spectroscopy, and valence band maxima were measured by x-ray photoelectron spectroscopy. Bandgaps determined from the differences are reproduced in Fig. 1, which shows the variation in silicon film thickness. Bandgaps for

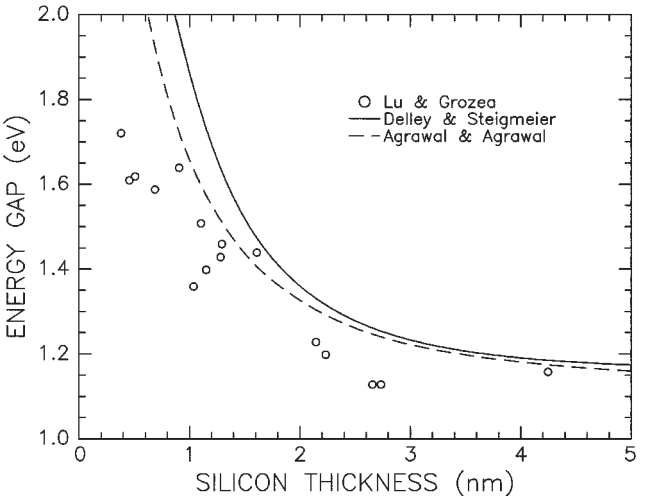

Fig. 1. The energy bandgaps in thin silicon films: measurements by Lu and Grozea[6] and theory curves interpolated and extrapolated from work of Delley and Steigmeier[4] and Agrawal and Agrawal.[7]

films thinner than 2.5 nm are significantly larger than for bulk Si. The variation of bandgap with film thickness qualitatively follows theoretical expectations. Two curves are also shown in Fig. 1, representing results of two theoretical calculations for thin silicon films with H-terminated surfaces (a wide bandgap termination analogous to interfaces with SiO_2). These are based on electron-density functional theory[4] and an ab initio theory of electron structure.[7] The theoretical bandgap increases with decreasing Si film thickness, either approximately as an inverse[4] or an exponential[7] function of film thickness. The experimental results demonstrate that an SOI process is a promising method for tuning the wavelength in silicon-based optoelectronic devices.

Reduced dimensionality in composite silicon-based materials is receiving considerable attention. First among them is porous silicon,[8] which has been studied extensively because of its visible photoluminescence and electroluminescence at room temperature. A notable milestone was the fabrication of porous silicon LEDs over 10 years ago.[9,10] Anodic oxidation of Si in an HF-containing solution, followed by an oxidizing anneal, produces 100-nm silicon grains embedded in an oxide matrix.[11] The material exhibits photoluminescence with 0.1% efficiency. Electroluminescence efficiency is 0.001%.[12] Light emission at 1.1 eV is attributed to the excitation of electrons and holes in the sub-oxide matrix and diffusive transport to the Si crystals, where they recombine to the photon.[12] Integration of a 0.1% efficiency, porous-silicon LED process with silicon electronic-driving circuits fabricated on a silicon wafer has also been demonstrated.[13]

Silicon crystals as small as 1 nm, embedded in an oxide matrix and denoted as nanocrystalline silicon, have been formed from silicon-rich oxide prepared by Si ion implantation, followed by anneal-

ing at temperatures in the range of 900–1,100°C. Theoretically, quantum confinement could increase the bandgap to about 2.5 eV in a 2-nm nanocrystal.[4] Photoluminescence in the visible (755 nm or 1.65 eV) has been observed for such nanocrystalline material.[14]

Recently, optical gain was observed in a nanocrystalline sample prepared by a similar process to form ~3-nm silicon quantum dots at a density of 2×10^{19} cm^{-3}; the effect was attributed to radiative states associated with the Si/SiO_2 interface.[15] Pump radiation at 390 nm causes electron transfer from the highest occupied molecular orbital (HOMO) at the nanocrystal valence-band edge to the lowest unoccupied molecular orbital (LUMO) at the nanocrystal conduction-band edge. Fast nanosecond time-scale relaxation to an interface state leads to a population inversion. Slow microsecond time-scale relaxation from the interface state allows stimulated emission at 800 nm with a net modal gain (optical gain less absorption) of about 100 cm^{-1} produced by the device.

A tunneling metal-oxide semiconductor (MOS) diode fabricated with nanocrystalline silicon grown by SiH_4/N_2O chemical-vapor deposition and annealing at temperatures in the range of 1,100–1,250°C was shown to exhibit electroluminescence at ~850 nm.[16] The silicon nanoparticles have mean radii of 1–1.8 nm and are present in concentrations of 39–46%. The light emission in the device originates from electron-hole recombination in the Si nanocrystals under Fowler–Nordheim and direct tunneling. Tunneling superlattice structures comprised of alternating layers of nanocrystalline Si and SiO_2 are also being investigated for the development of quantum superlattice devices.[17]

Strain induced by nanofabrication of GeSi quantum dots and superlattices can induce lattice distortions that change the symmetry properties of electronic wave functions in a manner not realized by quantum confinement in itself.[18] Lattice strain can transform the lowest interband transitions to induce direct gap behavior, thereby opening up the possibility of eliminating phonon-mediated recombination.[19]

Nanowires (also known as nanorods and nanowhiskers) have received much attention in the literature. The porous-Si etching method was used to fabricate free-standing silicon nanowires that exhibit photoluminescence in the visible (red), which was attributed to an increase in the bandgap.[20] Structures have also been fabricated with compositional modulation along the nanowire length (i.e., one-dimensional superlattices).[21] Single-crystal nanowires comprising of a Si/Si-Ge superlattice have been grown by a hybrid method of pulsed laser ablation and chemical-vapor deposition using Au clusters on SiO_2 to seed the growth.[22] Seeded chemical-vapor deposition has also been used to grow modulation-doped, Si p-n superlattice wires. Twenty-nanometer wide wires were fabricated into a two-terminal device to demonstrate the current-voltage characteristics of the p-n junctions.[23] Although they are still under development, nanowire-superlattice structures are deemed to hold potential for light-emission devices. This may include a quantum cascade laser. Recent progress in this area has been the observation of hole-intersubband electroluminescence at 132 meV observed (albeit at reduced temperature, $T < 180$ K) in p-type, planar quantum-cascade structures formed from 4-nm $Si_{0.68}Ge_{0.32}$ quantum wells.[24]

Inverse Photodiode

Owing to the reciprocity in the electron-hole-photon-phonon interaction, silicon diodes can serve as both photodetectors and LEDs. Light-emitting devices have been designed that resemble p-i-n diodes, avalanche photodiodes, and solar cells.

The p-i-n photodiode is operated in reverse bias and collects photogenerated minority carriers. A silicon p-i-n photodiode that is commercially available (Hamamatsu (Hamamatsu Photonics, Hamamatsu City, Japan) S5971 type with ~300-μm i-layer) was shown to produce 1.1-eV electroluminescence from bimolecular recombination at room temperature under forward bias.[25] The quantum efficiency was about 0.01%, and the response time was about 200 ns, which was determined for pulsed current operation under a reverse bias.

The avalanche diode has a high field region that produces additional electron-hole pairs that amplifies the photogenerated current. High-efficiency and high-speed avalanche photodetectors have been fabricated with an n+p−i−p+ structure[26] and a PtSi Schottky barrier structure.[27] Operating such devices at avalanche-breakdown reverse bias leads to photon emission.[28] Silicon avalanche photodetectors that are compatible with standard complementary metal-oxide semiconductor (CMOS) fabrication technology have been integrated into circuits.[29] Such devices emit light in the spectral range of 500–650 nm and are deemed to have potential for on-chip and chip-to-chip optical links, owing to brightness that is a factor of 10^3 or greater than the noise threshold of Si p-n photodetectors that would be used in an integrated communication system. Multiple-terminal silicon LED devices have been used to control the light emission (which is a strong function of bias) from avalanche devices.[30] In a demonstration of the potential for signal processing, a 14×14 matrix of gated n+p LEDs was integrated into a CMOS circuit (0.8-μm, bipolar CMOS technology) to produce an all-silicon optoelectronics system. The light-emission intensity, which is linear in the avalanche current, was controlled by gate bias (nonlinear dependence) in the resistive-gate Si LED matrix. Avalanche diode LEDs may, therefore, have applications in planar, light-emitting electro-optic interfaces in standard CMOS technology.

Optical Confinement

In solar cells, light trapping by means of surface texturing and roughness is used to increase the

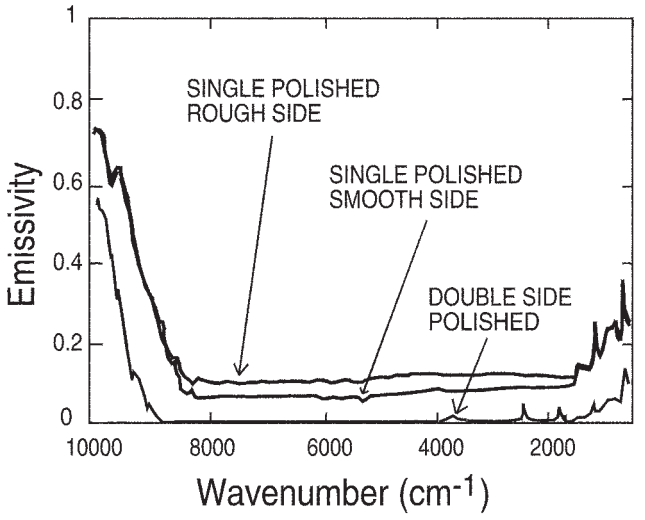

Fig. 2. The spectral emissivities of the rough and smooth sides of a single-side polished Si wafer and of a double-side polished Si wafer.[32]

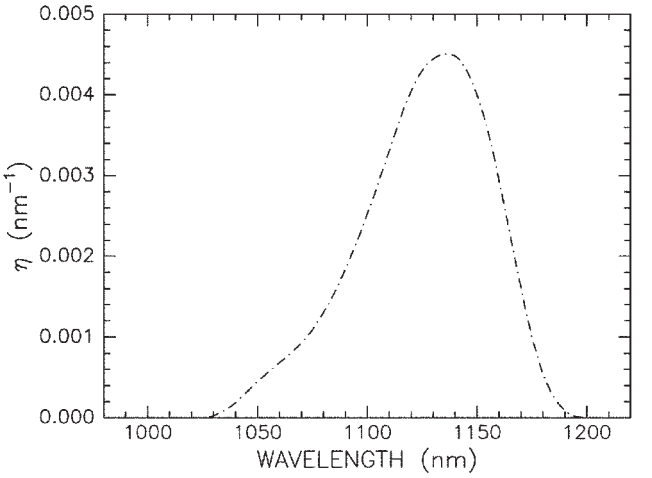

Fig. 3. The calculated, differential quantum-coupling efficiency between solar-cell-type LED and photodetector diodes.[34]

effectiveness of the silicon as an optical absorber. Ray optics theory has been used to model and optimize this optical confinement effect for random and periodically rough surfaces.[31] Surface texture is thus employed in solar cells to enhance the absorptivity to incident radiation. Part of the light incident on a rough silicon surface undergoes multiple internal total reflections, which increases the effective absorptivity. The effect is readily demonstrated by measurements of the optical properties of a silicon slab that is polished on one side to produce a smooth surface and etched on the other side to produce a rough surface (typical of single-side polished, crystalline-Si wafers). Figure 2 shows the spectral hemispherical emissivity (integrated over 2π solid angle of incident radiation) of two 0.65-mm-thick Si wafers (doping $n \sim 10^{15}$ cm^{-3}), one single-side polished and the other double-side polished. Emissivity, ε, is determined from the expression $\varepsilon = 1 - R - T$, where R and T are the measured reflectivity and transmissivity, respectively.[32] By optical reciprocity, the absorptivity is determined by the emissivity. The surface texture in the single-side polished wafer (10–30 μm laterally, 1-μm rms vertically) is seen to increase the emissivity. Moreover, in the mid-infrared region, the emissivity of the rough side is larger than the emissivity of the polished side.

Solar-Cell-Type Light-Emitting Diode

A solar-cell design optimized for high efficiency (24.7%) was applied to produce a high-efficiency silicon LED (0.85% power-conversion efficiency).[33] Surface texture was optimized for light trapping in the Si LED by etching inverted-pyramid arrays on the surface. Surface passivation with SiO_2 to maximize the surface recombination velocity and an antireflection coating were also used. Further, the quantum efficiency of bimolecular recombination was maximized by using float-zone silicon with high minority-carrier lifetime (~1 ms) and small area diffused p+ back-surface field contacts.

A 2 cm × 2 cm LED with light output peaking at 1,155 nm was placed next to a similar diode (2-mm gap between the two). Photodetection response cuts off above 1,200 nm.[34] The convolution between the LED emission and the photodetector absorption curves peaks near 1,135 nm, as shown in Fig. 3. The integrated collection quantum efficiency is 33%. The experiment reported a relatively high, optical-coupling quantum efficiency of 0.18%, defined as the ratio of the photodiode collector-current density to the LED current density (quasi-static measurement). At low operating-power density (<1 mW/cm^2), the power efficiency of a Si LED was shown to exceed that of a commercial GaAlAs LED (Opto Diode (Opto Diode, Newbury Park, CA) TO39). This is attributed to the $n = 1$ ideality factor shown by the current-voltage characteristic of the Si diode at low operating-current density ($J < 10$ mA/cm^2). Nonradiative recombination dominates at low current density in the GaAlAs LED, as revealed by a current-voltage characteristic that yields $n = 2$ and that leads to lower efficiency at low power.

Coupling efficiency in an all silicon-based communications system, which would also involve a modulator, could be optimized by reducing the bandgap of the photodetector through increased Si doping concentration, alloying with Ge, or by a strained epitaxial-layer method.

Carrier Confinement

In principle, light-emission efficiency can be boosted by carrier confinement by means of nanostructures, such as mentioned in the previous section. Spatial confinement of the electrons and holes would promote exciton formation, and thus, light emission would arise from a two-particle exciton-phonon interaction. Several methods have recently been employed to achieve room-temperature light emission through carrier confinement.

Near lasing action has recently been reported in an MOS tunneling structure where the insulating layer was a spun-on film of ~12-nm SiO_2 particles.[35] The metal electrode was a deposited Al film that conforms to the texture of the dielectric. Under bias, the nonuniformity of the dielectric thickness causes lateral inhomogeneity in the Si band bending. This, it is argued, leads to electron and hole confinement near the interface. A device that exhibited a current threshold for light emission also exhibited resonance modes in the electroluminescence spectrum. There were numerous noise-like peaks, the major ones being separated by about 4.5 nm and are strongest in the region near 1,140 nm. A device without a current threshold exhibits a smooth electroluminescence spectrum peaking at about 1,140 nm. The resonant cavities were presumed to involve reflection from the backside Al contact. This experiment appears to foreshadow the likelihood that lasing action can be realized in silicon with perhaps more precise experimental control over the current injection and cavity geometries and reduce the influence of nonradiative defect centers.

Another technique involving carrier confinement to produce electroluminescence takes advantage of the dislocation loops formed in silicon by ion implantation and annealing.[36] A p-n junction (~200-nm deep) was formed in n-type Si ($n \sim 10^{15}$ cm^{-3}) by implanting 30-keV B at a 10^{15} cm^{-2} dose and annealing for 20 min at 1,000°C. Dislocation loops are formed near the implant range (~100 nm) in the p+ diffusion region. The technique differs from dislocation-rich p-n junctions formed by laser recrystallization, which show room-temperature electroluminescence at ~1.6 μm (~10^{-6} external efficiency) and are attributed to dislocation-related D1 centers.[37] Although defects cause significant junction leakage at reverse bias, the diodes emit light under forward bias (1,160-nm peak at room temperature, 0.1% estimated quantum efficiency, 180-μs response time). Increases in the bandgap (20–750 meV) caused by the strain fields near the dislocation loops is argued to create carrier confinement and to be responsible for light emission.

The depth of the dislocations loop array can also be positioned more optimally relative to the p-n junction by using multiple implant and annealing technique, such as that developed for shallow junction formation.[38] To test this, silicon was prepared with a diffused n-type well (5×10^{15} cm^{-3} P); followed by a 30-keV 10^{15} cm^{-2} Si pre-amorphization implant; and a 5-keV, 5×10^{15} cm^{-2} B doping implant.[39] The B dopant was activated (sheet resistance: 266 Ω/sq, hole carrier density: 5.6×10^{14} cm^{-2}) by solid-phase epitaxial regrowth at 600°C, producing a junction at a depth of 24 nm and an array of dislocation defects at a depth of 60 nm (mean size 36 nm and average density 8×10^{10} cm^{-2}). Photoluminescence is observed at room temperature, as shown in Fig. 4, despite the very high density of nonradiative recombination defects that cause reverse-bias junction leakage (inset; leakage is 12 mA/cm^2 at –1 V bias and depletion depth ~50 nm). The spectrum shows peaks at 1,150 nm corresponding to transverse-optical (TO) phonons and at 1,210 nm corresponding to TO plus transverse-acoustic phonons. Rapid thermal annealing can be employed to reduce junction leakage (e.g., 7-$\mu A/cm^2$ leakage after a 900°C, 30-sec anneal).

A summary of peak energies obtained for band-to-band recombination photo- and electro-luminescence in various experiments[11,25,33,36,39] on silicon devices

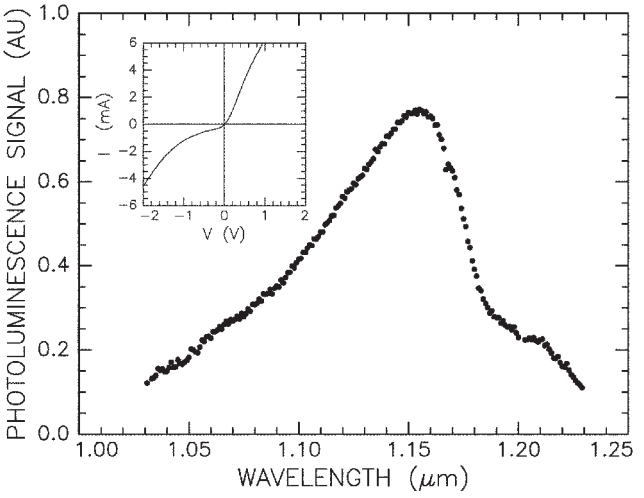

Fig. 4. The room-temperature photoluminescence of a shallow p-n junction diode (Si:B-Si:P) formed by Si preamorphization, B implantation, and solid-phase epitaxial regrowth. Inset: diode current-voltage curve.

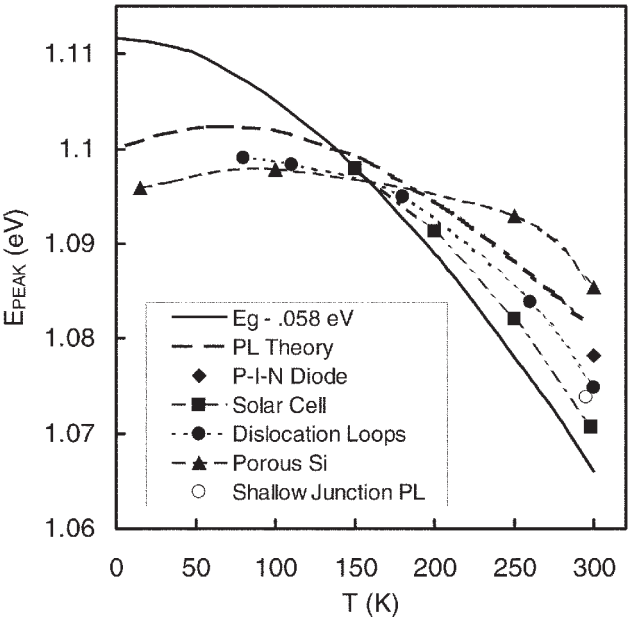

Fig. 5. The plot of the energy gap of silicon, reduced by the 58-meV TO phonon energy (solid curve) and theoretical photoluminescence energy (dashed curve).[11] Data are peak energies of electroluminescence in a p-i-n diode,[25] a solar-cell-type LED,[33] dislocation loop LED,[36] porous silicon LED,[11] and of photoluminescence in a shallow p-n junction.[39]

are plotted as symbols in Fig. 5. The solid curve, which shows the temperature dependence of the difference between the energy gap in silicon and the energy of the TO phonon (58 meV), is a good qualitative description of the trends in the data. The dashed curve represents the theoretical, photoluminescence peak energy.[11]

DEFECT-MEDIATED LIGHT EMISSION

Depletion Layer Impurities

There have been numerous experiments on luminescent defects in silicon. For example, focused ion-beam implantation in SOI was used to produce white-electroluminescent nanostructure, lateral npn-diodes in SOI.[40] Light emission in the range 400–650 nm was attributed to current-driven, microplasma excitation of oxygen-related defects in the crystalline Si layer.

Impurity-related defects in the depletion region of a silicon p-n junction has been used to produce light emission. Electronic transitions at 1.5 μm in the partially filled 4f shell of Er^{3+} ions in silicon has been used for LEDs of up to 0.01% efficiency[41,42] and for waveguide detectors of up to 0.1% efficiency.[43] The highest LED efficiencies were observed in n^+-p^+ devices doped with Er in the depletion layer and operated with reverse bias, where the Er ions are excited by hot carriers with radiative response times under 10 μs.[44] Although efficiencies are low, work in this area is stimulated by goals for all- silicon optoelectronic systems that exploit the optical transparency of Si and silica fibers at 1.5 μm. For such applications, an all-silicon optical modulator has been designed around a bipolar-mode, field-effect transistor integrated with a rib Si waveguide.[45] An electrically pumped Er-doped Si LED was proposed for the amplifier in this technology design, and the feasibility of laser action by its insertion between two Bragg reflectors was studied theoretically.[46]

Electroluminescence at 1.5 μm has been observed in diodes with β-$FeSi_2$ precipitates in the p-type region formed by ion implantation and annealing.[47] As with Er-doped Si LEDs (forward biased), the quantum efficiency is probably insufficient (<0.01% at room temperature) for general applications, owing to high nonradiative recombination at room temperature in these defect systems.[48,49]

Luminescence in SiOx

Silicon-rich oxides (SiO_x, $x < 2$) have been used to make luminescent media. Oxygen deficiency centers in SiO_2 films, produced by Si, Ge, or Sn ion implantation and furnace or rapid thermal annealing, have been used to generate blue-violet emission in electroluminescent devices with 0.025–0.05% efficiencies.[50] Electroluminescence is explained by mechanisms that include field ionization of the luminescent centers, electron trapping, and impact excitation by hot electrons and radiative recombination. Nanocrystalline surface states were the proposed explanation for the luminescent properties of 3-nm Si particles that were synthesized by ion implantation of wet-growth thermal oxide and annealing.[51] Low threshold-voltage LEDs were produced, operating in the hopping (non-Fowler–Nordheim) regime at electric fields below 5 MV/cm without hot carrier injection.

Rare-earth luminescence centers in nanoparticles have greater efficiencies than in bulk silicon and thus hold significant promise for silicon-based light-emitting devices. Importantly, the presence of silicon nanoparticles has been found to increase the Er excitation cross section relative to a pure oxide host. Hot electron injection through a sub-oxide layer was used to excite Er centers in silicon nanoparticles within an oxide matrix in a p-Si/$SiO_{1.6}$/Si:Er:O/n-Si structure grown by molecular-beam epitaxy (540°C).[52] The sub-oxide injector boosted the external quantum efficiency under reverse-bias operation at room temperature, by about a factor of 2, to 0.013% (internal quantum efficiency 0.3%). Erbium-doped silicon nanocrystals have also been grown by plasma-enhanced chemical-vapor deposition of the sub oxide, followed by annealing at 1,250°C.[53] Using a microcavity, a sharp photoluminescence at 1.54 μm was observed.

Competing nonradiative de-excitation of impact-ionized Er in SiO_x has been a stumbling block against boosting the light-emission efficiency much above 0.1%, preventing competition with group III-V compound semiconductors. Recently, MOS devices with SiO_x implanted with Er were reported to have a much higher quantum efficiency, up to 10% for $x = 2$, which is both a remarkable advance compared to previous work and approaches that of standard LEDs made with III-V materials.[54] Experimental MOS devices were fabricated with an n^+-poly-Si/Er:SiO_x/epi-p-Si/p^+-Si structure. The epitaxial layer is 22 μm, and the oxide is either 62-nm thermal SiO_2 or 70-nm SiO_x grown by plasma-enhanced chemical-vapor deposition. Erbium is introduced in the oxide with a 50 keV, 10^{15} cm^{-2} implant, followed by 30-min anneal at 800°C. The gate electrode is 300-nm n^+ polycrystalline Si, which is transparent to the emitted radiation at 1,540 nm. For structures with $x = 2$ (thermal oxide), the maximum radiated power reaches 1.6 mW/cm^2, which is limited by saturation of excited Er atoms. The radiative decay lifetime was determined to be 3 ms and the excitation cross section to be 10^{-14} cm^{-2}. The Er ions increase the charge-to-breakdown of the oxide, which is attributed to hot electron-energy loss caused by collisions with Er ions. Deposited silicon-rich oxides are even more robust with respect to charge-to-breakdown criteria, but the light emission is also reduced by an increase in nonradiative loss. The optimum materials are silicon-rich oxides with a low excess of Si and an index of refraction $n < 1.61$. The quantum efficiency is about 1%, which is determined by a tradeoff of high efficiency and high charge to breakdown. Similar MOS LEDs implanted with Tb show light emission at 550 nm. Other rare implants are Yb (983 nm) and Ce.

SILICON-BASED LUMINESCENT DEVICES

Nanocrystalline silicon fabricated by a porous silicon process (current-modulated anodization under illumination and rapid thermal oxidation or chemical oxidation) has been used as an emitter of ballistic electrons.[55] A thin Au film was used as the acceleration electrode to demonstrate electron emission and to determine the spectra of the electrons emitted into vacuum. The peak energy is about half the bias voltage, and the maximum energy is about 5 eV less than the bias voltage (bias up to 15 V). The mean distance between electron traps in the porous silicon is estimated to be 2 μm at high bias. A planar luminescent device was prepared by vacuum deposition of a visible luminescent organic material, Alq_3 (green peak emission at 540 nm, 40-ns time constant). A thin transparent Au film is used as the top electrode. The ballistic electrons excite the HOMO to LUMO transitions in the Alq_3 film, which radiatively decay. Such devices are being considered as vacuum-less cathode ray tubes that can be used to produce multicolor displays.

Another approach for a silicon-based display technology appeals to the well-established techniques of plasma excitation and phosphors, such as those in fluorescent lighting. Figure 6 is an illustration of a pressurized, plasma display pixel, which is suitable for integration with silicon electronic circuits.[56,57] Electrical conductors are fabricated in the silicon to form a cross point separated by a hollow cavity adjacent to an open tube. The volume is filled with pressurized gas and is excited by an applied voltage above the Paschen minimum firing voltage, emitting ultraviolet (UV) radiation. Phosphor coatings on the tubes are used to convert the UV emission to visible light. The technology is used to produce multicolor displays.

APPLICATIONS

A silicon light-emitting device, depending on the technology configuration, will be used in conjunction with a modulator as the light source for massively parallel optical interconnects, e.g., between processor and memory and peripherals as well as within processors. A modulator will be a necessary requirement for such applications because high efficiency remains incompatible with rapid response, owing to the indirect Si bandgap. The advantages are globally low power dissipation; low-area input/output connections beyond pin limitations; shortened, effective electrical-wire lengths; high speed; high aggregate bandwidth; and low latency. One could anticipate silicon chips with combined optical and electronic processing. The LEDs, such as those based on the rare-earth implanted silicon-rich oxides, could find applications in low-cost electro-optical isolators. The applications are in optical signaling, for use in hostile environments with high electric and magnetic fields, and for three-dimensional optoelectronic systems.

The feasibility of all-optical integrated circuits built in silicon will depend on a suitable silicon light emitter.

Visible luminescent devices, briefly reviewed here, would have applications in displays and, given fabrication and operating costs, could find applications in electric lighting, signaling, and photodynamic therapies.[58]

One can also envision potential applications in micromechanical and chemical sensors. Chemically sensitive, field-effect transistors are currently being investigated for the detection of biological and chemical species, for example, with nanowire sensors.[59] The sensitivity and identification analysis uses an electrical measurement of conductance or capacitance. The addition of a light source could broaden the scope of such applications (enzyme activity, for example) by introducing an optical excitation probe (and detector). Figure 7 is a schematic illustration of a nanobiosensor that integrates an optical source with the electrical detectors.

CONCLUSIONS

The mechanisms of light emission from silicon include high-efficiency bandgap emission; bandgap modifications; quantum confinement; carrier confinement; light trapping; defect and interface states; hot-carrier tunneling; and avalanche breakdown.

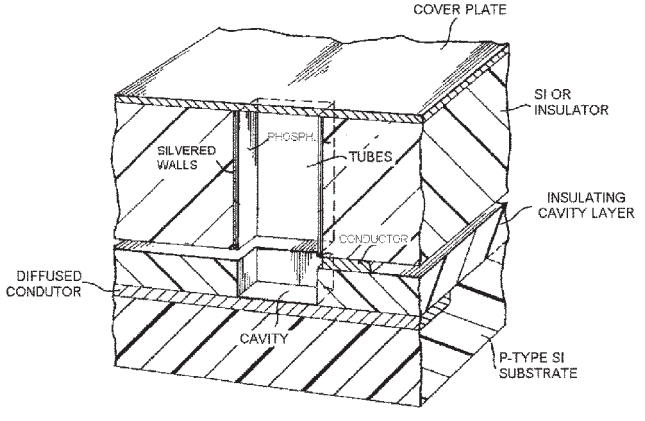

Fig. 6. A cut-away view of a pixel element for a plasma display built in silicon.[56]

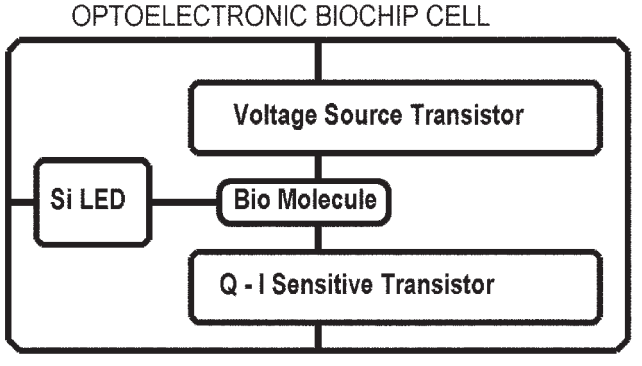

Fig. 7. A schematic illustration of integration of a silicon LED for optical excitation in molecular and biosensor electronics.

The materials for component devices include silicon-rich oxide with Si nanoparticles or rare-earth dopants, porous silicon, silicon-germanium nanostructures, rare-earth-doped bulk silicon, thin-film silicon on oxide, semiconductor species, and doping superlattices.

The trend is toward nanostructured materials. Currently, this is dominated by matrix-composite materials with largely random nanostructure. Given the trend from microelectronics to nanoelectronics, exemplified by the 10-nm fin-field-effect transistor recently fabricated in SOI with a modified, planar-CMOS process,[60] the viable technology for integrated, silicon light emitters is likely to evolve toward similarly defined nanostructures. This will allow building efficient light-emitting structures and optical pathways under holistic nano-architectural planning.

ACKNOWLEDGEMENTS

The authors acknowledge partial support from TMS and the New Jersey Institute of Technology.

REFERENCES

1. L. Scanlon, *Technol. Rev.* 106, 88 (2003).
2. E.F. Kingsbury and R.S. Ohl, *Bell System Technol. J.* 31, 802 (1952).
3. P. Ball, *Nature* 409, 974 (2001).
4. B. Delley and E.F. Steigmeier, *Appl. Phys. Lett.* 67, 2370 (1995).
5. S.S. Iyer, R.T. Collins, and L.T. Canham, eds., *Light Emission from Silicon,* Vol. 256 (Pittsburgh, PA: Materials Research Society, 1992).
6. Z.H. Lu and D. Grozea, *Appl. Phys. Lett.* 80, 255 (2002).
7. B.K. Agrawal and S. Agrawal, *Appl. Phys. Lett.* 77, 3039 (2000).
8. A. Uhlir, *Bell System Technol. J.* 35, 333 (1956).
9. R.T. Collins, P.M. Fauchet, and A.M. Tischler, *Phys. Today* 50, 24 (1997).
10. B. Das and S.P. McGinnis, *Semicond. Sci. Technol.* 14, 988 (1999).
11. L. Tsybeskov, K.L. Moore, D.G. Hall, and P.M. Fauchet, *Phys. Rev. B* 54, R8361 (1996).
12. L. Tsybeskov, K.L. Moore, S.P. Dattagupta, K.D. Hirschmann, D.G. Hall, and P.M. Fauchet, *Appl. Phys. Lett.* 69, 3411 (1996).
13. K.D. Hirschman, L. Tsybeskov, S.P. Dattagupta, and P.M. Fauchet, *Nature* 384, 338 (1996).
14. S. Guha, M.D. Pace, D.N. Dunn, and I.L. Singer, *Appl. Phys. Lett.* 70, 1207 (1997).
15. L. Pavesi, L. Dal Negro, G. Mazzoleni, G. Franzò, and F. Priolo, *Nature* 408, 440 (2000).
16. G. Franzò, A. Irrera, E.C. Moreira, M. Miritello, F. Iacona, D. Sanfilippo, G. Di Stefano, P.G. Fallica, and F. Priolo, *Appl. Phys. A* 74, 1 (2002).
17. L. Tsybeskov, G.F. Grom, P.M. Fauchet, J.P. McCaffrey, J.-M. Baribeau, G.I. Sproule, and D.J. Lockwood, *Appl. Phys. Lett.* 75, 2265 (1999).
18. S. Froyen, D.M. Wood, and A. Zunger, *J. Electron. Mater.* 17, S11 (1988).
19. Y.S. Tang, S. Hicks, C.M. Sotomayor Torres, W.-X. Ni, C.D.W. Wilkinson, and G.V. Hansson, *Proc. SPIE* 3007, 170 (1997).
20. L.T. Canham, *Appl. Phys. Lett.* 57, 1046 (1990).
21. D. Appell, *Nature* 419, 553 (2002).
22. Y. Wu, R. Fan, and P. Yang, *Nano Lett.* 2, 87 (2002).
23. M. Gudiksen, L.J. Lauhon, J. Wang, D.C. Smith, and C.M. Lieber, *Nature* 415, 617 (2002).
24. G. Dehlinger, L. Diehl, U. Gennser, H. Sigg, J. Faist, K. Ensslin, D. Grützmacher, and E. Müller, *Science* 290, 2277 (2000).
25. T. Dittrich, V.Y. Timoshenko, J. Rappich, and L. Tsybeskov, *J. Appl. Phys.* 90, 2310 (2001).
26. H. Melchior, A.R. Martman, D.P. Schinke, and T.E. Seidel, *Bell System Technol. J.* 57, 1`791 (1978).
27. H. Melchior, M.P. Lepselter, and S.M. Sze, *IEEE Solid-State Device Res. Conf.* (Boulder, CO, 17–19 June 1968).
28. A.G. Chynoweth and K.G. Mckay, *Phys. Rev.* 102, 369 (1956).
29. L.W. Snyman, H. Aharoni, M. du Plessis, J.F.K. Marais, D. van Niekerk, and A. Biber, *Opt. Eng.* 41, 3230 (2002).
30. M. du Plessis, H. Aharoni, and L.W. Snyman, *IEEE Photonic Technol. Lett.* 14, 768 (2002).
31. E. Yablonovitch, *J. Opt. Soc. Am.* 72, 899 (1982); B.L. Sopori and T. Marshall, *Conf. Record 23rd Photovoltaic Specialists Conf.* (Piscataway, NJ: IEEE, 1993), pp. 127–132.
32. N.M. Ravindra, B. Sopori, O.H. Gokce, S.X. Cheng, A. Shenoy, L. Jin, S. Abedrabbo, W. Chen, and Y. Zhang, *Int. J. Thermophys.* 22, 1593 (2001); S. Abedrabbo, J.C. Hensel, A.T. Fiory, B. Sopori, W. Chen, and N.M. Ravindra, *Mater. Sci. Semicond. Process.* 1, 187 (1998).
33. M.A. Green, J. Zhao, A. Wang, P.J. Reece, and M. Gaf, *Nature* 412, 805 (2001).
34. J. Zhao, M.A. Green, and A. Wang, *J. Appl. Phys.* 92, 2977 (2002).
35. C.-F. Lin, P.-F. Chung, M.-J. Chen, and W.-F. Su, *Opt. Lett.* 27, 713 (2002).
36. W.L. Ng, M.A. Lourenço, R.M. Gwilliam, S. Ledain, G. Shao, and K.P. Homewood, *Nature* 410, 192 (2001).
37. E.Ö. Sveinbjörnsson and J. Weber, *Appl. Phys. Lett.* 69, 2686 (1996).
38. J.O. Borland, T. Matsuda, and K. Sakamoto, *Solid State Technol.* 45, 83 (2002).
39. A.T. Fiory, J.O. Borland, H.-J. Gossman, C.S. Rafferty, J.L. Benton, and C. Lindfors, unpublished research.
40. H. Röchen, J. Meijer, A. Stephan, U. Weidenmüller, H.H. Bukow, and C. Rolfs, *Nucl. Instrum. Methods B* 181, 275 (2001).
41. B. Zheng, J. Michel, F.Y.G. Ren, L.C. Kimerling, D.C. Jacobson, and J.M. Poate, *Appl. Phys. Lett.* 64, 2842 (1994).
42. S. Coffa, G. Franzò, and F. Priolo, *Appl. Phys. Lett.* 69, 2077 (1996); S .Coffa, G. Franzò, F. Priolo, F.A. Pacelli, and A. Lacaita, *Appl. Phys. Lett.* 73, 93 (1998).
43. P.G. Kik, A. Polman, S. Libertino, and S. Coffa, *J. Lightwave Technol.* 20, 862 (2002).
44. S. Coffa, G. Franzò, and F. Priolo, *Appl. Phys. Lett.* 69, 2077 (1996).
45. A. Sciuto, S. Libertino, A. Alessandria, S. Coffa, and G. Coppola, *J. Lightwave Technol.* 21, 228 (2003).
46. S. Coffa, S. Libertino, G. Coppola, and A. Cutolo, *IEEE J. Quant. Electron.* 36, 1206 (2000).
47. D. Leong, M. Harry, K.J. Reeson, and K.P. Homewood, *Nature* 387, 686 (1997).
48. C. Spinella, S. Coffa, C. Bongiorno, S. Pannitteri, and M.G. Grimaldi, *Appl. Phys. Lett.* 76, 173 (2000).
49. F. Priolo, G. Franzò, S. Coffa, and A. Carnera, *Phys. Rev. B* 57, 4443 (1998).
50. L. Rebohle, T. Gebel, J. von Borany, H. Frob, D. Borchert, and W. Skorupa, *Mater. Sci. Eng. C* 19, 373 (2002); L. Rebohle, J. von Borany, H. Fröbb, T. Gebel, M. Helm, and W. Skorupa, *Nucl. Instrum. Methods B* 188, 28 (2002).
51. J. De La Torre et al., *Physica E* 16, 326 (2003).
52. M. Markmann, A. Sticht, F. Bobe, G. Zandler, K. Brunner, G. Abstreiter, and E. Müller, *J. Appl. Phys.* 91, 9764 (2002).
53. D. Pacifici, A. Irrera, G. Franzò, M. Miritello, F. Iacona, and F. Priolo, *Physica E* 16, 331 (2003).

54. M.E. Castagna, S. Coffa, M. Monaco, L. Caristia, A. Messina, R. Mangano, and C. Bongiorno, *Physica E* 16, 547 (2003).
55. Y. Nakajima, A. Kojima, and N. Koshida, *Appl. Phys. Lett.* 81, 2472 (2002).
56. M.P. Lepselter, U.S. patent 5,954,560 (21 September 1999).
57. K.C. Choi, G.F. Saville, and S.C. Lee, *IEEE Trans. Electron Dev.* 45, 1356 (1998).
58. N. Lane, *Sci. Am.* 288, 38 (2003).
59. Y. Cui, Q. Wei, H. Park, and C.M. Lieber, *Science* 293, 1289 (2001).
60. B. Yu et al., 2002 *Int. Electron Devices Meeting Digest* (Piscataway, NJ: IEEE, 2002), pp. 251–254.